



Water-induced surface reconstruction of oxygen (2×1) covered Ru(0001)

Sabine Maier,¹ Pepa Cabrera-Sanfelix,² Ingeborg Stass,^{1,3} Daniel Sánchez-Portal,^{2,4}
Andrés Arnau,^{2,4,5} and Miquel Salmeron^{1,6,*}

¹Materials Sciences Division, Lawrence Berkeley National Laboratory, Berkeley, California 94720, USA

²Donostia International Physics Center, Paseo Manuel de Lardizabal 4, San Sebastian 20018, Spain

³Institut für Experimentalphysik, Freie Universität Berlin, Arnimallee 14, 14195 Berlin, Germany

⁴Centro de Física de Materiales, Materials Physics Center (MPC), CSIC-UPV/EHU, Paseo Manuel de Lardizabal 5,
San Sebastian 20018, Spain

⁵Departamento de Física de Materiales, Facultad de Química, UPV/EHU, Apdo. 1072, San Sebastian 20080, Spain

⁶Department of Materials Science and Engineering, University of California–Berkeley, Berkeley, California 94720, USA

(Received 30 April 2010; published 20 August 2010)

Low-temperature scanning tunneling microscopy and density-functional theory (DFT) were used to study the adsorption of water on a Ru(0001) surface covered with half monolayer of oxygen. The oxygen atoms occupy hcp sites in an ordered structure with (2×1) periodicity. DFT predicts that water is weakly bound to the unmodified surface, 86 meV compared to the ~ 200 meV water-water H bond. Instead, we found that water adsorption causes a shift of half of the oxygen atoms from hcp sites to fcc sites, creating a honeycomb structure where water molecules bind strongly to the exposed Ru atoms. The energy cost of reconstructing the oxygen overlayer, around 230 meV per displaced oxygen atom, is more than compensated by the larger adsorption energy of water on the newly exposed Ru atoms. Water forms hydrogen bonds with the fcc O atoms in a (4×2) superstructure due to alternating orientations of the molecules. Heating to 185 K results in the complete desorption of the water layer, leaving behind the oxygen-honeycomb structure, which is metastable relative to the original (2×1) . This stable structure is not recovered until after heating to temperatures close to 260 K.

DOI: [10.1103/PhysRevB.82.075421](https://doi.org/10.1103/PhysRevB.82.075421)

PACS number(s): 68.43.Bc, 68.37.Ef

I. INTRODUCTION

Understanding water-solid interfaces is important in a variety of phenomena including catalysis, electrochemistry, and corrosion. It has also major applications in hydrogen production and fuel cells. Water adsorption on clean single crystalline metal surfaces was intensively investigated by various experimental techniques as a model system for understanding water-solid interfaces. In ambient conditions, metal surfaces interact with a vast number of molecules, among others oxygen and water. Thus most metal surfaces are covered by an oxide film and a water layer whose thickness depends on the relative humidity. Chemisorbed oxygen on metal surfaces forms well ordered and atomically flat overlayers and are therefore ideal surfaces to study the initial interaction of water molecules with surface oxygen.

Co-adsorbed oxygen is known to change the dissociation behavior of water on Pt-group metal surfaces significantly. On Ru(0001) (Refs. 1–4) and other Pt-group metals⁵ it was shown that the adsorption of water changes as a function of oxygen coverage. Dissociation is observed at low oxygen coverage ($\theta < 0.2$ ML) while it is inhibited at larger O coverage ($\theta = 0.25$ – 0.5 ML) contrary to studies that assume that water remains intact when interacting with oxygen.^{6–9} Pre-adsorbed oxygen on the ruthenium surface does not only influence the dissociation characteristics of water but also its structure. On the $p(2 \times 2)$ oxygen terminated surface, water adsorbs in a $p(2 \times 2)$ symmetry,^{4,10} compared to a hexagonal arrangement ($\sqrt{3} \times \sqrt{3}$) $R30^\circ$ observed on clean hexagonal-close-packed metal surfaces.^{11–13}

Unlike the open $p(2 \times 2)$ -O surface, the denser $p(2 \times 1)$ -O surface leaves much less room for the water to

adsorb because all the preferred adsorption sites, i.e., atop sites, are blocked. Older results suggested that the high oxygen coverage on Ru(0001) (Ref. 6) as well as on Ni(111) (Ref. 14) and Rh(111) (Ref. 15) prevents any long-range ordering in the water overlayer. Recently, Gladys *et al.*¹ performed an x-ray photoelectron spectroscopy (XPS) and near-edge x-ray absorption spectroscopy (NEXAFS) study of water adsorption on the $O(2 \times 1)/\text{Ru}(0001)$ surface. They reported that water adsorbs intact at 140 K and no indication of dissociation was observed at higher temperatures near the point of desorption. Although these measurements did not provide the local geometry of water on the $p(2 \times 1)$ -O surface, based on steric and symmetry arguments the authors proposed that water orders in a honeycomb structure, (2×2) - $(2O-H_2O)$, where half of the oxygen atoms from the $O(2 \times 1)$ overlayer shift from hcp sites to fcc sites [see Fig. 7(b)]. Such a structure enables water to adsorb on the preferred metal top sites. The formation of a honeycomb O structure has previously been observed in adsorption experiments of CO (Refs. 16–18) and NO (Refs. 19–21) on the $p(2 \times 1)$ oxygen covered ruthenium surface. The XPS experiments of Gladys *et al.*¹ showed that between 170 and 180 K most of the water desorbs intact from the surface and that the binding energy of the O 1s peak of the remaining water changed by 0.6 eV, indicating the formation of a second water species $H_2O(2)$. Recently, Shavorskiy *et al.*²² reported that the intact water species adsorbed on the $O(2 \times 1)/\text{Rh}(111)$ surface between 160 and 190 K have the same spectroscopic signature in XPS as the one observed for higher oxygen coverage on Ru(0001). Therefore, they assume that these adsorption states are in similar geometries on both surfaces. This indicates that the oxygen-honeycomb

structure, which has top sites available for the water molecules to adsorb, might not only form on oxygen precovered ruthenium but also on other metal surfaces as well upon water adsorption.

So far, model calculations and direct experimental evidence for the formation of the oxygen-honeycomb structure upon adsorption of water on the $O(2 \times 1)/\text{Ru}(0001)$ surface are missing. In this paper, we present a study of the adsorption of water on $\text{Ru}(0001)$ precovered with 0.5 ML of oxygen, based on low-temperature scanning tunneling microscopy (STM) and density-functional theory (DFT) calculations. Our experiments and calculations confirm the formation of the honeycomb structure driven by the adsorption of water. We discuss the local geometry of water and oxygen in detail. In particular, we found that the water molecules form a superstructure with (4×2) periodicity due to the alternation of two preferred molecular orientations.

II. EXPERIMENTAL METHOD

The experiments were performed using a homebuilt low-temperature scanning tunneling microscope operated in ultrahigh vacuum (UHV) (base pressure $<5 \times 10^{-11}$ Torr). The $\text{Ru}(0001)$ surface was cleaned by repeated annealing and cooling cycles between 770 and 1770 K in a partial oxygen atmosphere (4×10^{-8} Torr), in order to deplete the first subsurface layers from carbon contaminations. The remaining oxygen on the surface was removed by annealing the sample to 1720 K in UHV. A $p(2 \times 1)$ oxygen overlayer was prepared by exposing the clean surface to 60 L of oxygen at 820 K followed by 10 min annealing at 930 K.²³ After preparation, the sample was transferred to the STM station in a connected UHV chamber. Water was dosed *in situ* through a tubular doser at sample temperatures between 140 and 200 K. All STM images presented in this paper were acquired at 7 K.

III. THEORETICAL METHOD

Density-functional theory calculations were performed in order to determine the preferred configuration of the adsorbed water layer and on the related oxygen-honeycomb reconstruction. We have also investigated the energetics of the reconstruction process with and without water. The calculations were done using the Vienna package (VASP),^{24–26} within the Perdew-Wang 1991 version of the general gradient approximation.²⁷ The projector augmented wave^{28,29} method was used to describe the interaction of valence electrons with the Ru, O, and H cores. A symmetric slab of seven Ru layers and the same amount of vacuum was used to represent the $\text{Ru}(0001)$ surface. The oxygen and water adsorbates are placed on the top and bottom surfaces of the symmetric slab. A plane-wave cutoff of 400 eV and a $6 \times 6 \times 1$ k -point sampling were used for the smallest cell, corresponding to a (2×2) unit cell of the clean $\text{Ru}(0001)$ surface. For supercells of different sizes we used a similar k -sampling density. All the geometries were optimized by allowing relaxation of all degrees of freedom of the two outermost Ru layers and the O and H atoms until residual forces were

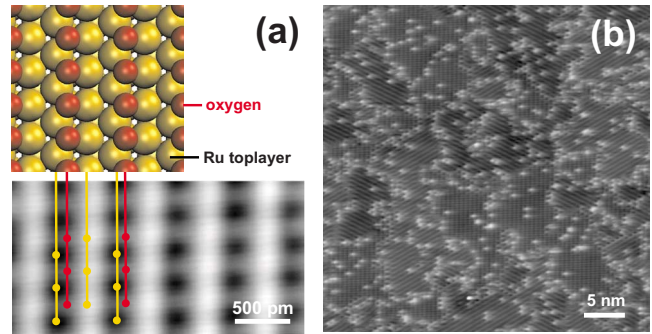


FIG. 1. (Color online) (a) Atommically resolved STM image (bottom) and schematic representation (top) of the $O(2 \times 1)/\text{Ru}(0001)$ surface. Red circles represent the oxygen atoms and yellow represent the Ru atoms. (b) Large scan area image of the $O(2 \times 1)/\text{Ru}(0001)$ surface, showing different domains rotated 120° with respect to each other. White spots correspond to O vacancies. Imaging parameters: [(a) and (b)] 21.5 mV and 89.6 pA.

smaller than $0.03 \text{ eV}/\text{\AA}$. Different sources of uncertainty, such as k -point sampling, plane-wave cutoff, and force convergence criteria were checked in previous calculations for water adsorption on $O(2 \times 2)/\text{Ru}(0001)$ substrate.³ The estimated absolute error bar for the adsorption energy of a water molecule is $\sim 10 \text{ meV}$ and thus it does not affect the conclusions of the paper regarding the reconstruction of the $O(2 \times 1)/\text{Ru}(0001)$ substrate. However this error bar is larger than the typical energy differences between structures with different molecular orientations, such as those presented in Sec. IV C 2. These energy differences are mostly governed by dipole-dipole interactions and thus are quite small. However, when comparing structures with different molecular orientations we can expect a strong cancellation of errors and the obtained results are, at least qualitatively and also probably semiquantitatively, significant. STM simulations based on the structures obtained by DFT were performed using the Tersoff-Hamann^{30,31} approximation, assuming constant current and a bias voltage of +400.0 mV.

IV. RESULTS AND DISCUSSION

A. $(2 \times 1)\text{O-Ru}(0001)$ surface

Prior to water adsorption we identified the different high-symmetry sites on the O-precovered surface that were later used to determine the water adsorption site. This is usually not trivial since the imaging contrast of the oxygen precovered surface is strongly voltage dependent.^{10,32} We found that our STM images compare well with previously published STM image calculations of the $O(2 \times 1)/\text{Ru}(0001)$ surface.³³ In Fig. 1(a) the individual oxygen atoms of the (2×1) rows are resolved. The corresponding surface geometry is schematically represented in the same figure for comparison. The oxygen atoms appear as dark depressions relative to the ruthenium surface.³⁴ A large scan image of the surface, Fig. 1(b), shows that the surface consists of different domains rotated by 120° with respect to each other. Our surface preparation leads to an averaged domain size of approximately 50 nm^2 and a concentration of O defects less than

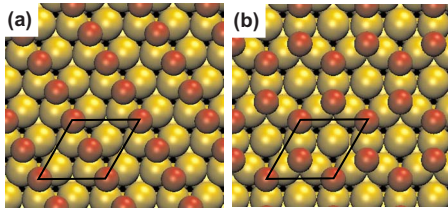


FIG. 2. (Color online) Structures formed by oxygen on Ru(0001) at half-monolayer coverage. Two possible surface geometries are shown, along with the (2×2) cell (dark lines) used in the DFT calculations. Yellow circles correspond to Ru atoms and red circles correspond to oxygen adsorbed on Ru hollow sites. (a) $O(2 \times 1)$ layer with all O atoms occupying hcp positions and (b) $2O(2 \times 2)$ honeycomb structure with half of the O atoms in hcp and half in fcc sites. Both systems were calculated and the $O(2 \times 1)$ structure found to be more stable by 231 meV per (2×2) cell.

20%. The surface imaged in Fig. 1(b) was slightly under dosed and the bright spots represent exposed Ru regions.

Figure 2 shows two possible high-symmetry structures of the 0.5 ML oxygen precovered Ru(0001) surface. In Fig. 2(a) the oxygen atoms sit on hcp sites arranged in a $O(2 \times 1)$ structure and in Fig. 2(b) the oxygen atoms form a honeycomb structure occupying both hcp and fcc sites. Our calculations show that the $O(\text{hcp})$ pattern [Fig. 2(a)] is the preferred configuration by ~ 231 meV per (2×2) cell, or per displaced O atom, compared to the honeycomb structure in Fig. 2(b). This energy difference indicates the preference of O atoms to adsorb on hcp sites. This is consistent with our STM observations that always showed the well-ordered $O(\text{hcp})$ structure after the preparation procedure outlined in Sec. II in the absence of water.

In the $O(2 \times 1)$ overlayer [Fig. 2(a)] the oxygen atoms adsorb 1.24 \AA above the Ru topmost layer. There are four Ru top layer atoms per unit cell: two of them are bound to two $O(\text{hcp})$ atoms and the other two are bound to only one oxygen atom. The Ru atoms adjoining two $O(\text{hcp})$ are pulled 0.08 \AA vertically toward the bound O atoms. This buckling of the first ruthenium layer, caused by the chemisorbed oxygen, as well as the oxygen-Ru distances are consistent with previous low-energy electron diffraction²³ and medium energy ion scattering experiments³⁵ as well as DFT calculations.^{33,36} In the $2O(2 \times 2)$ honeycomb structure [Fig. 2(b)] the $O(\text{hcp})$ atoms adsorb 1.22 \AA over the Ru topmost layer, whereas this height increases to 1.46 \AA for the $O(\text{fcc})$ atoms, i.e., 0.24 \AA higher. In this honeycomb structure, three of the four Ru top atoms in the unit cell are bound to two oxygen atoms and so slightly pulled from the surface. The fourth Ru atom is not bound to any oxygen, leading to a small buckling of the surface of about 0.11 \AA . As we will see below, this exposed top Ru atom creates the stable site for water adsorption.

Further calculations in a larger cell have been performed in order to determine the energy cost of the reconstruction as a function of the percentage of oxygen atoms displaced from hcp to fcc sites. Using a (4×4) unit cell, we found that the energy cost (ΔE) to move one (12.5% of the oxygen atoms in the surface moved, $\Delta E=185 \text{ meV/O}$), two (25%, $\Delta E=191 \text{ meV/O}$), three (37.5%, $\Delta E=212 \text{ meV/O}$), and

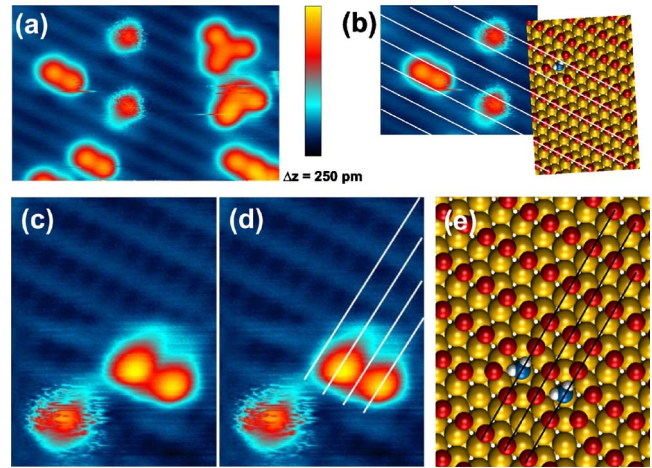


FIG. 3. (Color online) (a) STM image showing individual water molecules, and groups of two and three molecules in adjacent sites on a $O(2 \times 1)/\text{Ru}(0001)$ adsorbed at 140 K. During imaging at 7 K, clusters of neighboring molecules are stable while isolated molecules are vibrating. ($5.8 \text{ nm} \times 3.8 \text{ nm}$, -380 mV , and 5.4 pA). The schematic in (b) shows that water molecules adsorb between the oxygen rows. The Ru atoms are represented in yellow, surface oxygen in red, and the oxygen of the water molecule in blue. [(c) and (d)] Images showing isolated water molecules and pairs of molecules on a well resolved image of the $O(2 \times 1)/\text{Ru}(0001)$ surface ($2.9 \text{ nm} \times 4.7 \text{ nm}$, -245 mV , and 10 pA). The schematic drawing in (e) shows the location of the water molecules relative to the (2×1) oxygen lattice.

four (50%, $\Delta E=231 \text{ meV/O}$) oxygen atoms is roughly additive. Forming the honeycomb structure, i.e., displacing half of the oxygen atoms, costs $\sim 231 \text{ meV/O}$. This value progressively decreases, up to a $\sim 20\%$, as the percentage of displaced oxygen atoms is reduced.

B. Water monomers and small clusters

Figure 3(a) shows a STM image of the $O(2 \times 1)/\text{Ru}(0001)$ surface with a few water molecules adsorbed at 140 K. The molecules appear as $\sim 160 \text{ pm}$ protrusions above the $10\text{--}20 \text{ pm}$ corrugation of the oxygen overlayer. The edges of isolated molecules are fuzzy in the images for bias voltages between 150 and 380 mV, for both positive and negative voltages. Such fuzziness is not observed in molecules occupying contiguous sites. Since at temperatures below 40 K there is insufficient thermal energy for the water to diffuse freely on the surface, we surmise that the monomer is vibrationally excited by tunneling electrons. Below 150 mV the libration modes ($85\text{--}115 \text{ meV}$), the frustrated rotation or the Ru-OH_2 stretch mode ($\sim 48 \text{ meV}$) can be excited by the tunneling electrons.³⁷ In the case of molecules in neighboring sites these vibrations are inhibited due to the water-water interaction which stabilizes the relative orientation of the molecules. We will come back to this point of the preferred relative molecular orientations when considering the case of higher water coverage.

The image in Fig. 3(b) reveals that water molecules adsorb between the oxygen rows (dark lines). Figures 3(c) and 3(d) provide additional information since the (2×1) over-

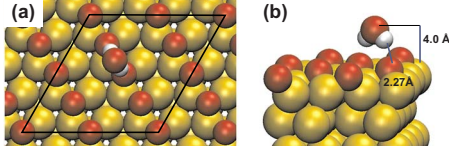


FIG. 4. (Color online) Optimized model of a hypothetical water molecule adsorbed on an unmodified $O(2 \times 1)/Ru(0001)$: (a) top view and (b) side view. Two quite long and weak hydrogen bonds are formed with the oxygen atoms in the surface. The calculated binding energy of 86 meV is insufficient to ensure wetting.

layer in the background is well resolved. These images show that the water molecules adsorb on top sites and that neighboring molecules are separated by two lattice spaces (measured distance: 533 ± 10 pm). Because the molecules adsorb on Ru top sites we conclude that the adsorption of one water molecule provides enough energy to reconstruct the underlying oxygen overlayer to create a free Ru top site.

These results are in contrast with another plausible adsorption configuration for water on $O(2 \times 1)/Ru(0001)$ that was proposed in Ref. 38. In this configuration, see Fig. 4, the molecular plane is vertical and two hydrogen bonds (H bonds) are established with two O atoms in the $O(2 \times 1)$ overlayer. Our calculations show that this configuration is weakly bound, with an adsorption energy of 89 meV per molecule. Water prefers to adsorb on Ru top sites if they are available and, as we will see in the following, in the case of the $O(2 \times 1)/Ru(0001)$ surface the water molecules are able to create such exposed top sites by displacing O atoms from their most stable adsorption site.

In order to explore different possibilities for the adsorption of water on the oxygen-honeycomb reconstructed surface, we used several geometries where one, two, three, and four oxygen atoms were moved from hcp to fcc sites in a (4×4) unit cell. The water molecule adsorbs always on exposed Ru top sites, with its oxygen located 2.23 \AA above the

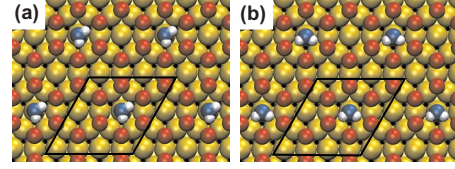


FIG. 5. (Color online) Models of water adsorption structures on the $2O(2 \times 2)/Ru(0001)$ honeycomb surface. A 4×4 cell (marked by the lines) was used for the calculations. The coverage of water is 0.25 ML. Yellow circles correspond to Ru atoms. Red circles correspond to oxygen atoms at hcp and fcc sites; the oxygen of the water molecule is represented in blue. The difference between the two structures is the orientation of the water molecule: (a) H atoms point toward the O(hcp) atoms and (b) H atoms point toward the O(fcc) atoms. Adsorption energies are given in the last row of Table I. The O(fcc)-oriented molecules are ~ 60 meV more stable.

Ru atom and slightly displaced ($\sim 0.2 \text{ \AA}$) in the xy plane relative to the Ru top position in order to facilitate the formation of H bonds with neighboring O atoms in the substrate. The molecule has two different orientations depending on whether the OH bonds point toward O(hcp) or O(fcc) sites. For the fully reconstructed oxygen-honeycomb structure the two possible orientations are shown in Fig. 5. In the configuration shown in Fig. 5(a) two H bonds are formed with neighboring O(hcp) atoms, whereas in the other orientation [Fig. 5(b)] the molecule is bound to the closest O(fcc) atoms. The H bonds with O(fcc) atoms are ~ 30 meV stronger than those formed with O(hcp) atoms. They are also shorter, 2.30 \AA compared to 2.46 \AA . Therefore, configurations in which the hydrogen atoms of the molecule point toward O(fcc) atoms are ~ 60 meV more stable than those with an O(hcp) orientation. The adsorption energies for all the studied configurations are shown in Table I. Notice that in all cases the adsorption energy on the reconstructed surface (in the range 0.8–1 eV) is around ten times larger than on the original $O(2 \times 1)/Ru(0001)$ surface (configuration

TABLE I. Adsorption energy (E_{ads}) of one water molecule on a partially reconstructed (4×4) supercell of the $O(2 \times 1)/Ru(0001)$ surface. As indicated in the first column, E_{ads} is given for different fractions of oxygen atoms displaced to fcc sites. The (hcp) and (fcc) labels correspond to different orientations of the water molecule with the hydrogen atoms oriented, respectively, toward O_{hcp} or O_{fcc} atoms, E'_{ads} is the adsorption energy relative to the clean unreconstructed $O_{\text{hcp}}(2 \times 1)/Ru(0001)$.

	E_{ads} [relative to the reconstructed $O/Ru(0001)$] (meV)	E'_{ads} [relative to the unreconstructed $O_{\text{hcp}}(2 \times 1)/Ru(0001)$] (meV)
12.5% O shifted to fcc	788 (hcp) ^a	603 (hcp) ^a
	821 (fcc) ^a	636 (fcc) ^a
25.0% O shifted to fcc	885 (hcp)	503 (hcp)
	937 (fcc)	555 (fcc)
37.5% O shifted to fcc	966 (hcp)	330 (hcp)
	1023 (fcc)	387 (fcc)
50.0% O shifted to fcc	977 (hcp)	53 (hcp)
	1034 (fcc)	110 (fcc)

^aFor the 12.5% configurations the hydrogen bonds are always formed with O(hcp) atoms. Here, fcc and hcp labels refer to the orientation of the plane bisecting the molecule. This plane passes through the closest O(fcc) atom for the so-called fcc configuration.

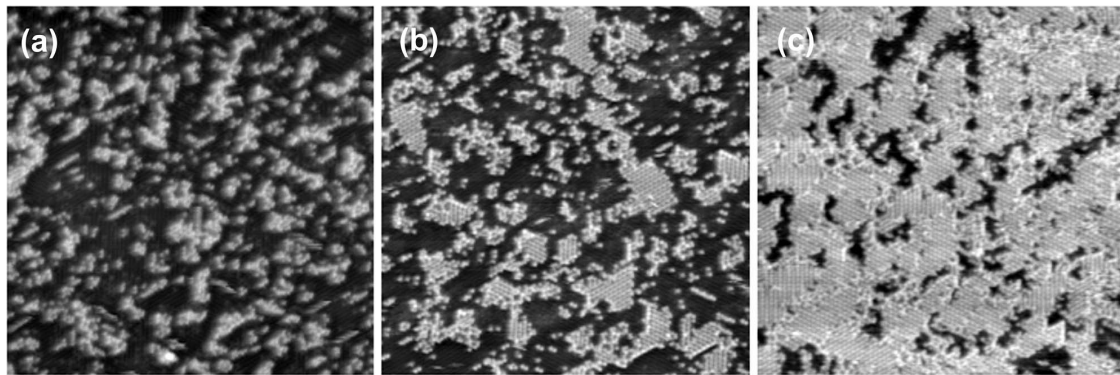


FIG. 6. STM images of the $O(2 \times 1)/Ru(0001)$ surface with different amounts of water adsorbed at 140 K: (a) 10–20 % (b) 20–30 %, and (c) 75–85 % water coverage. All images are $40 \text{ nm} \times 40 \text{ nm}$ in size. STM image parameters: (a) -155 mV and 37 pA , (b) 221 mV and 8 pA , and (c) -385 mV and 4 pA .

shown in Fig. 4). Furthermore, the adsorption energy increases significantly (by more than 200 meV) as more oxygen atoms shift to fcc sites. Therefore, the energy released by the adsorption of a single water molecule compensates the energy cost to displace up to four oxygen atoms from hcp to fcc sites ($\sim 231 \text{ meV}$ per oxygen atom). This clearly justifies the viability of the formation of the oxygen-honeycomb structure after adsorption of water.

C. Water cluster formation

1. Water structures after adsorption at 140 K

Figure 6 shows STM images of the O-covered Ru(0001) surface after adsorption of different amounts of water, starting from around 10% up to about 85% of the saturation coverage. The molecules form ordered domains on top of the O-covered substrate. These domains have higher contrast in STM images (bright in the figures) than the uncovered oxygen (2×1) areas. The formation of domains indicates that water-water interactions play a decisive role in the arrangement of the molecules. As the water coverage grows the water domains expand to cover most of the surface, shown in

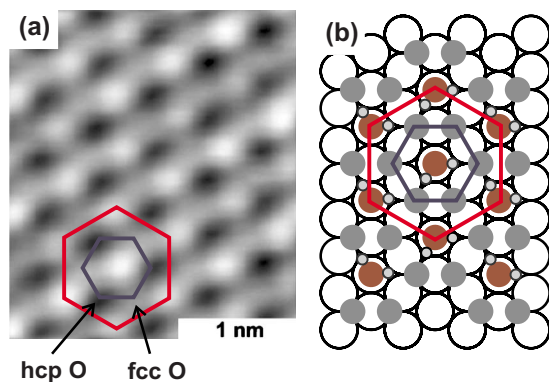


FIG. 7. (Color online) (a) High-resolution STM image from a water domain revealing the hexagonal structure of the adsorbed water. (b) Model structure of showing water adsorbed on the $2O(2 \times 2)/Ru(0001)$. Adapted from Ref. 1. STM image parameters: (a) 221 mV and 8 pA , and (b) 221 mV and 7 pA .

Fig. 6(c), indicating that the first water layer wets the surface. We assume the water adsorbs intact as there is no evidence for water dissociation even when heating the sample at higher temperatures, see Sec. IV E.

Figure 7(a) shows an expanded view of an area inside an ordered water domain, with individual water molecules (brightest spots) resolved. The molecules form a hexagonal structure, in agreement with the model proposed by Gladys *et al.*¹ The image shows the different contrast of hcp and fcc oxygen atoms, the former appearing lower (darker) than the fcc ones. The same imaging contrast of fcc and hcp oxygen was observed in STM image simulations, see Fig. 10.

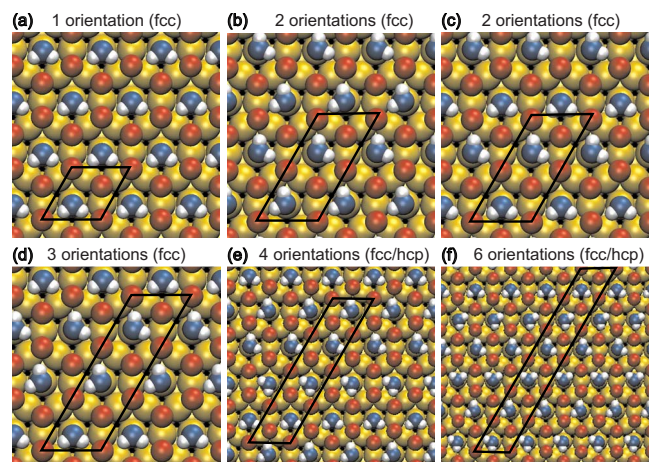


FIG. 8. (Color online) Overview of relaxed geometries from the DFT calculations for different relative orientations of the water molecules within the layer. (a)–(d) correspond to different configurations in which all the molecules are H bonded to O(fcc) atoms. In panel (e) one molecule out of four is H bonded to two O(hcp) atoms and in panel (f) 50% of the molecules are H bonded to O(hcp) atoms. In (a) all water dipoles are aligned while in (b) their directions alternate. These two configurations are the most stable and are energetically degenerated, with an adsorption energy $E_{\text{ads}}=896 \text{ meV}/\text{H}_2\text{O}$. The other configurations are slightly less stable with adsorption energies lower by $21 \text{ meV}/\text{H}_2\text{O}$ for (c), $17 \text{ meV}/\text{H}_2\text{O}$ for (d), $28 \text{ meV}/\text{H}_2\text{O}$ for (e), and $35 \text{ meV}/\text{H}_2\text{O}$ for (f).

2. Orientation of the water molecules within a cluster

In the following, we discuss the influence of the water-water interactions on the preferred orientation of the water molecules. For this study we performed calculations using supercells with sizes from (2×2) to (2×12) in units of the Ru(0001) unit cell. There are up to six possible orientations of a single water molecule in the oxygen-honeycomb structure. Three of these orientations correspond to configurations in which the molecule is H bonded to O(fcc) atoms while the other three orientations have the water molecule bound to O(hcp) atoms.

We first consider a configuration [Fig. 8(a)] where all the water molecules have the same orientation. The binding energy of this structure is 62 meV/H₂O higher if the molecules are H bonded to O(fcc) atoms than when they bond to O(hcp) atoms. This is agreement with the data in Table I (notice, however, that the data in Table I correspond to lower water coverage) and confirms the ~ 30 meV additional stabilization for each O(fcc)-oriented H bond respect to the O(hcp) ones. In the case of two different alternating orientations of the molecules, we have considered two configurations [Figs. 8(b) and 8(c)] formed by O(fcc)-oriented molecules. The configuration in Fig. 8(b) is energetically degenerate with that in panel (a). However, the structure in Fig. 8(c), where the water dipoles make angles of 60° and face each other in pairs of rows, is ~ 21 meV/H₂O less stable than the optimum dipole-parallel water rows in Fig. 8(a). The energy ordering of these structures can be fully understood from the interaction between the dipoles of the adsorbed molecules. Taking into account only the dipole-dipole interaction the structure in panel (a) is the most stable followed closely by (b). Structure (c) has a lower adsorption energy. More specifically, the difference between the dipole-dipole interaction energy of structures (a) and (c) is more than six times higher than the corresponding difference for configurations (a) and (b). Interestingly, a starting geometry similar to that in Fig. 8(b) but formed by O(hcp)-oriented molecules was not stable during optimization and spontaneously evolved to the configuration shown in Fig. 8(a). This confirms the strong preference of the water molecules in this substrate for the H bonding to O(fcc) atoms.

We have also considered a configuration [Fig. 8(d)] of O(fcc)-oriented molecules with three different relative orientations of water in successive rows. This structure is less stable (by ~ 17 meV/H₂O) than the optimal configurations in Figs. 8(a) and 8(b). Again, this is consistent with the energetics derived from dipole-dipole interactions.

We can also consider more than three relative orientations among the water molecules but then at least one molecule per cell has to be H bonded to O(hcp) atoms. This will reduce the stability of these structures by ~ 60 meV per molecule. Hence, it should be energetically unfavorable to have more than three orientations within a cluster. This is confirmed by our calculations. As expected, the configuration with four different water orientations, with one imposed O(hcp)-oriented molecule out of four [see Fig. 8(e)], is less stable by 28 meV/H₂O compared to the optimal configurations in Figs. 8(a) and 8(b). An alternative configuration with four different water orientations: 50% O(hcp)/50% O(fcc)-

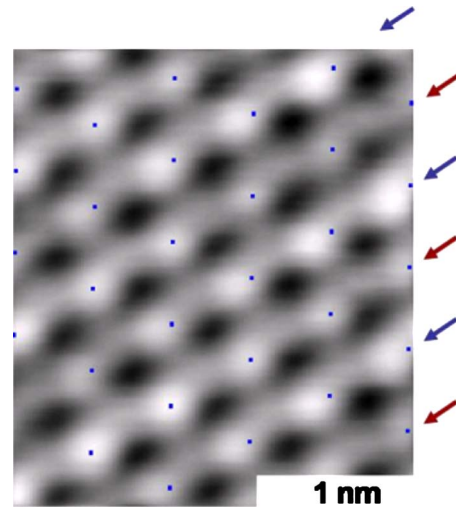


FIG. 9. (Color online) Experimental STM image showing the presence of slight deviations from the perfect (2×2) alignment in the position of the maxima corresponding to water molecules, represented by the blue lattice. Every second row is slightly displaced.

oriented molecules are also less stable than the optimum ones by ~ 30 meV/H₂O. Figure 8(f) shows a configuration with six relative water orientations in which half of the molecules are O(hcp) oriented. This configuration has a 35 meV/H₂O lower adsorption energy than the most stable ones.

In summary, the energy ordering of all the calculated structures can be explained as the result of dipolar intermolecular interaction with an adsorption energy penalty of 60 meV per O(hcp)-oriented molecule. Our calculations clearly show that the energy difference between O(fcc)-oriented and O(hcp)-oriented adsorption configurations of water in this substrate is larger than the energy differences associated with different relative orientations of the molecular dipoles. Therefore, at low temperatures we should only expect to find O(fcc)-oriented molecules in the oxygen-honeycomb reconstructed surface.

Experimentally we find that in some domains the water molecules do not show the same contrast and that their position deviates slightly from the perfect (2×2) alignment, as shown by the lattice of blue points in Fig. 9. In the molecular rows marked by red arrows the dots are centered over the water molecules while in the rows marked with blue arrows they are slightly off-centered. This asymmetry is not present in the oxygen-honeycomb structure obtained after desorbing the water above 185 K, which will be discussed later (Fig. 12). This observation suggests that the deviations from the perfect (2×2) structure are correlated with the orientation of the molecules. Simulated STM images corresponding to the three more stable configurations in Fig. 8 are presented in Figs. 10(d)–10(f). In the case of two and three relative water orientations, the STM simulations show that the center of the molecules is slightly displaced, similar to the shift observed in the experimental images. From this comparison we can conclude that two relative orientations of water molecules are indeed present in the experimentally observed configuration which, therefore, form to a (4×2) periodicity. This is

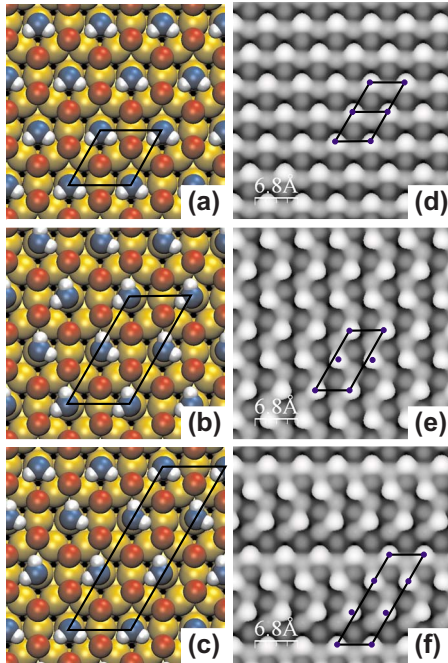


FIG. 10. (Color online) [(a)–(c)] Optimal configurations for the adsorption of water molecules on the oxygen-honeycomb reconstruction showing (a) one, (b) two, and (c) three different molecular orientations. Structures (a) and (b) are energetically degenerate while (c) is slightly less optimal by ~ 17 meV/ H_2O . In all the configurations, the water molecules are slightly displaced (~ 0.2 Å) along the xy plane, with respect to the Ru top sites, in order to form hydrogen bonds with the O(fcc) atoms (bond length 2.25 Å). [(d)–(f)] Corresponding simulated constant current images at +400 mV bias. In panels (e) and (f) the slightly displaced centers of the molecular protrusion are marked in blue.

supported by the fact that such molecular arrangement is calculated to be the most stable one, together with that in Fig. 8(a). Curiously, the energetically equivalent structure, where all the molecules are oriented in the same direction, has not been observed in the STM experiments. This indicates that, in reality, the structure with two alternating orientations and (4×2) periodicity is more stable than that with all the molecules aligned. However, the reason behind this larger stability is still unclear.

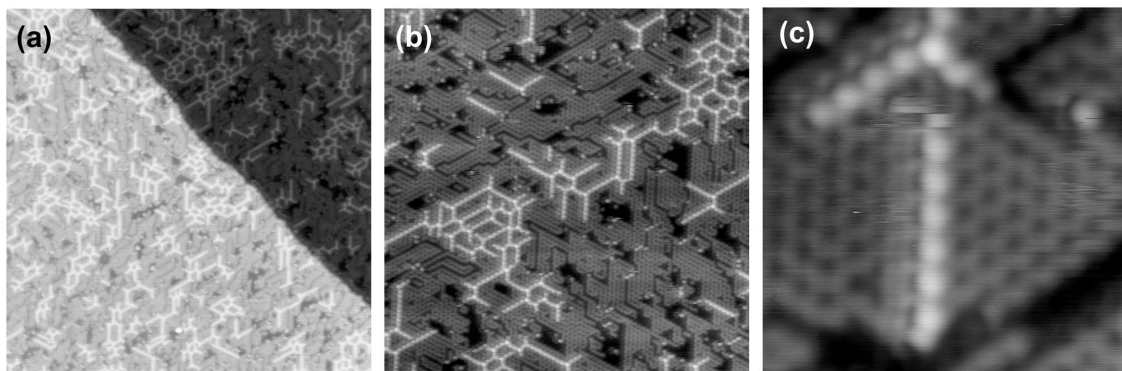


FIG. 11. Water adsorbed at 140 K on the O/Ru(0001) surface followed by annealing to 180 K. The residual water molecules form lines several nanometers long. The lines do not grow over monatomic steps nor decorate them as seen in (a). Image parameters: (a) 80 nm^2 , -340 mV, and 9 pA, (b) 40 nm^2 , -310 mV, and 5.5 pA, and (c) 6.6 nm^2 , -309 mV, and 5.4 pA.

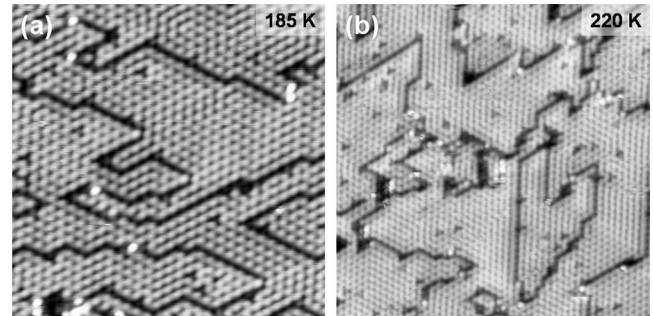


FIG. 12. STM images of the oxygen-honeycomb structure after desorbing the water by annealing to (a) 185 K ($15 \text{ nm} \times 15 \text{ nm}$) and (b) to 220 K ($25 \text{ nm} \times 25 \text{ nm}$). Image parameters: (a) -148 mV and 11 pA, and (b) -312 mV and 26 pA.

D. Water structures formed after annealing above 180 K

Annealing a nearly fully water covered surface [as that in Fig. 6(c)] to 180 K caused most of the water to desorb. A small residue of molecules were left on the surface forming one molecule wide lines several nanometers long, as shown in Fig. 11. These water lines were homogeneously distributed over the surface and have an apparent height of 55–65 pm over the oxygen covered ruthenium surface. The lines often start or end at an edge of underlying oxygen domains. The molecule at the junction of individual lines showed higher contrast than the rest of the water molecules, as shown in Fig. 11(c). The lines did not decorate the steps nor grew over monatomic steps. Interestingly, the oxygen overlayer around the lines retained the honeycomb structure and did not changed to the original $\text{O}(2 \times 1)$ structure. We will describe the characteristics of this honeycomb structure in further detail in the next section. In order to grow more of these water lines we dosed water while keeping the surface at 180 K. However, the coverage did not increase significantly. Annealing the sample to 185 K, even in the presence of background water, resulted in the complete desorption of the water layer and only the oxygen overlayer remained on the ruthenium surface, as shown Fig. 12(a).

The water lines could well correspond to the $\text{H}_2\text{O}(2)$ species identified by Gladys *et al.*² by XPS. Between 170 and 180 K these authors showed that most of the water desorbed

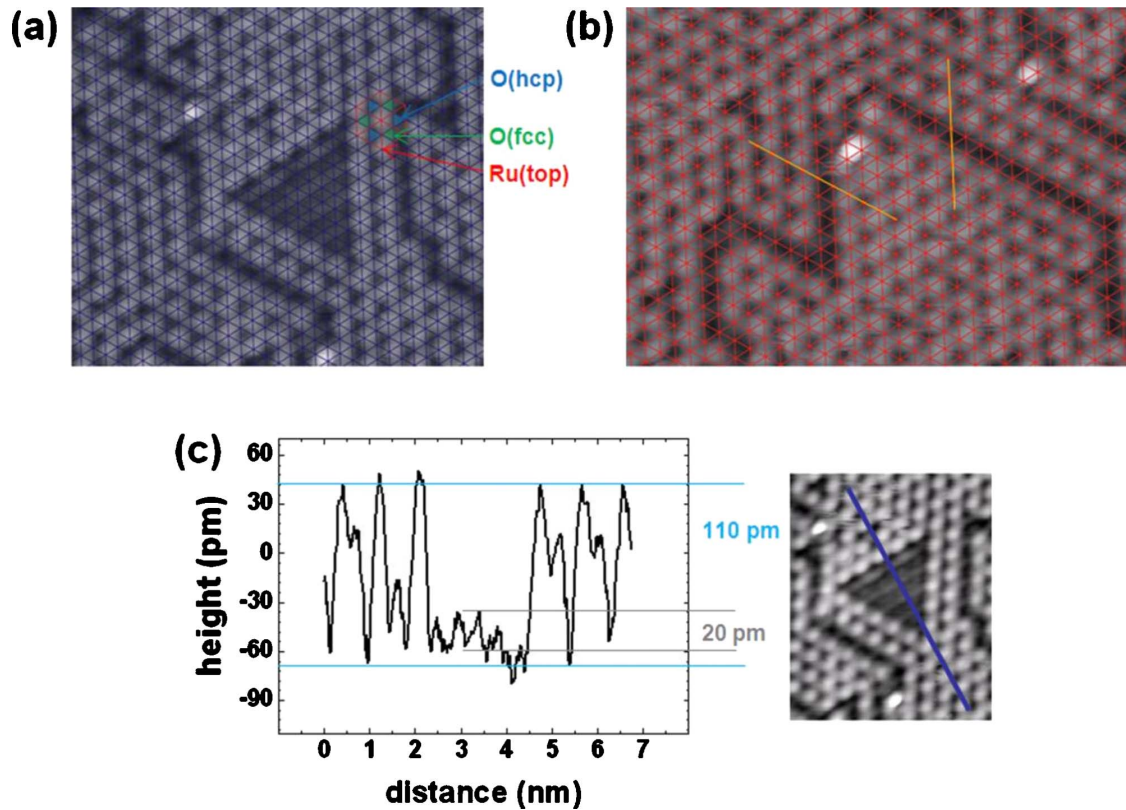


FIG. 13. (Color online) (a) High-resolution image ($9.2 \text{ nm} \times 6.8 \text{ nm}$) of the O honeycomb structure with a small patch of the original $O(2 \times 1)$ structure. The resolution of the images in the $O(2 \times 1)$ patch is sufficient for identification of the adsorption sites in the surrounding honeycomb structure. The nodes of the superimposed lattice located over the white protrusions in the honeycomb structure represent Ru(0001) top sites. (b) The dark stripes are domain boundaries between different honeycomb patches as can be seen more clearly with the help of the yellow lines. The nodes of the lattice in (b) represent Ru(0001) fcc sites ($9 \text{ nm} \times 5.2 \text{ nm}$). (c) Section through the $O(2 \times 1)$ patch and honeycomb structure in the right image, showing that the corrugation in the honeycomb structure is about five times higher than in the $O(2 \times 1)$ structure. According to the simulated STM images, the double peak structure might be attributed to the O(fcc) and Ru top atoms. STM parameters: -21 mV and 11 pA .

from the surface and the binding energy of O $1s$ peak of the remaining water changed by 0.6 eV , forming a second water species $\text{H}_2\text{O}(2)$, with a saturation coverage of 0.23 ML . We observed a slightly smaller coverage, which might be due to the difficulty of growing extended layers at these temperatures. They also concluded, using NEXAFS, that these water molecules are tilted with respect to the surface plane. At present, neither our STM experiments nor our simulations point in this direction. For water adsorbed on the $O(2 \times 2)/\text{Ru}(0001)$ surface, previous STM experiments in our group showed a tendency for the molecules to form short linear row structures at intermediate coverage, rather than denser two-dimensional patches.¹⁰

Manipulation experiments on individual water molecules using voltage pulses suggest that the molecules are not adsorbed in the domain boundaries between oxygen-honeycomb domains, as shown in Fig. 13(b). A possible explanation for the formation of water lines is that at 180 K the diffusion of water molecules competes with desorption allowing the water to arrange in thermodynamically favored structures. Thus, dipole-dipole interaction between the water molecules might cause the formation of linear water stripes.

E. Honeycomb-oxygen structure

The honeycomb-oxygen structure created by water adsorption remained unchanged after heating to 220 K [Fig. 12(b)]. The original $O(2 \times 1)$ surface, consisting of three different domains rotated by 120° with respect to each other,

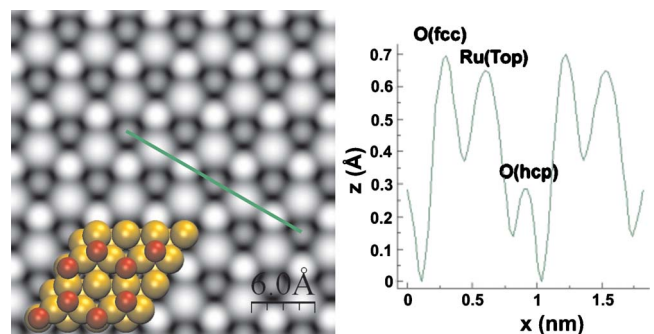


FIG. 14. (Color online) Calculated constant current STM image at $+400 \text{ mV}$ bias and topographic profile for the oxygen-honeycomb reconstruction. Inset: red circles correspond to O atoms and yellow circles correspond to Ru atoms.

was observed by STM after heating the surface to 260 K. Hence, the oxygen switches back from the fcc sites to the hcp sites to restore the original $O(2 \times 1)$ at around 260 K. The formation of oxygen-honeycomb structures starting from a $p(2 \times 1)$ oxygen covered ruthenium surface has also been observed with CO (Refs. 16–18) and NO.^{19–21} Regeneration of the $O(2 \times 1)$ structure by switching oxygen back from fcc sites to hcp sites was observed in conjunction with the desorption of CO and NO at 360 K for CO (Refs. 16–18) and 470 K for NO.²¹ Since desorption of these molecules occurs at a higher temperature than for water, it is not possible to prepare a pure oxygen-honeycomb structure without them. In contrast, the oxygen-honeycomb structure remains on the surface after the water desorption. The asymmetry in the temperatures of transformation of the two oxygen structures, with the $2O(2 \times 2)$ restructuring back to the $O(2 \times 1)$ at a measurably fast rate only above 260 K indicates the existence of an activation barrier separating these two structures. The catalytic role of water is crucial for the initial switching, reducing the barrier and stabilizing the $2O(2 \times 2)$ phase. Once water desorbs above 180 K, the hexagonal $2O(2 \times 2)$ structure is kinetically stabilized by the barrier. From the temperature where the transformation was observed we estimate the barrier to be around 0.5–0.7 eV.

The interesting metastable oxygen-honeycomb structure might be used as a template for the adsorption of other small molecules providing the unique feature of two kinds of oxygen species (fcc and hcp bound) compared to the other known oxygen reconstruction. Because the fcc oxygen is more weakly bound to the surface, it is also likely to be more reactive toward other coadsorbed molecules adsorbed at hcp sites.

The high-resolution image in Fig. 13(a) reveals dark patches between the honeycomb structures with the original $O(2 \times 1)$ structure. They correspond to residual areas not covered with water as in Fig. 6(c). We used these $O(2 \times 1)$ patches as a reference to identify the adsorption sites in the honeycomb structure. The white protrusions correspond to Ru top sites, the core of the honeycomb structure. The narrow dark stripes between honeycomb structures show also a (2×1) structure, qualitatively with the same contrast as the (2×1) patches. These stripes are domain boundaries between different honeycomb patches as can be seen in Fig. 13(b). The high-resolution images of the oxygen-honeycomb structure in Figs. 12 and 13 show no evidence for water dissociation, only a few defects/adsorbates are observed after water desorption. This is in agreement with Gladys *et al.*^{1,2} who reported water dissociation is suppressed on the $O(2 \times 1)/\text{Ru}(0001)$ surface as indicated by the absence of a OH peak in XPS.

We observed a significant larger corrugation, by about a factor 5, in the images of the honeycomb structure compared to that in the $O(2 \times 1)$. The corrugation of the $O(2 \times 1)$ is between 10 and 20 pm while the corrugation on the honeycomb structure can be up to around 100 pm, see Fig. 13(c). Large corrugations reflect a larger difference in the local density of states between O sites and Ru sites in the honeycomb structure. The corrugation of the $O(2 \times 1)$ structure is in agreement with previous experiments and calculations,³³ which described that the (2×1) structure has about a factor

3 weaker corrugation in STM images than the (2×2) . Our simulation of an STM image of the oxygen-honeycomb reconstruction is shown in Fig. 14. The simulated image reveals a corrugation of about 75 pm, confirming that the corrugation is large compared to that of the $O(2 \times 1)$ and $O(2 \times 2)$ structures.

V. CONCLUSION

In conclusion, STM experiments have shown that water adsorbs on the $O(2 \times 1)/\text{Ru}(0001)$ surface forming a well-ordered (4×2) superstructure at temperatures of 140 K. This requires displacement of half of the surface oxygen from an hcp to an fcc site to form a honeycomb structure that provides Ru top sites for the adsorption of water. DFT calculations have determined that binding of the water molecule to the unmodified $O(2 \times 1)/\text{Ru}(0001)$ structure is too weak to lead to wetting. Instead a reconstruction of the $O(2 \times 1)$ into a honeycomb $2O(2 \times 2)$ structure takes place that is driven by water adsorption. The energy cost of ~ 231 meV/oxygen atom for this reconstruction is well compensated by the adsorption of water on the exposed Ru atoms. At low coverage, water adsorbs strongly on top of the Ru atoms with its plane nearly parallel to the surface and with the hydrogen atoms oriented toward the oxygen atoms in the fcc-hollow sites. At low water coverage (0.0625 ML) the adsorption energy can be as high as $E_{\text{ads}} \sim 1.03$ eV/ H_2O , high enough to overcome the energy cost of moving four oxygen atoms from hcp to fcc sites in a (4×4) unit cell. At the saturation water coverage of 0.25 ML, we found two energetically degenerate configurations with $E_{\text{ads}} = 896$ meV/ H_2O . These structures differ in the relative orientation of the water molecules: in one configuration all the molecules are aligned while in the other the molecules alternate their orientations forming a (4×2) periodicity. Simulated STM images of these configurations show that the water molecules are slightly displaced (~ 0.2 Å), with respect to their Ru adsorption sites, toward the O(fcc) atoms with which they form H bonds. The STM images showed slight deviations in the position of the water molecules from a perfect (2×2) alignment, distorting it into a (4×2) periodicity, with two orientations of water molecules.

At 180 K, most of the water desorbed from the surface and the remaining water arranged in linear structures. Water was completely desorbed above 185 K, leaving behind a metastable oxygen-honeycomb structure. Only after heating to 260 K did the stable original (2×1) form again at a rate high enough to be observed.

ACKNOWLEDGMENTS

This work was supported by the Office of Basic Energy Sciences, Division of Materials Sciences and Engineering of the U.S. DOE under Contract No. DE-AC02-05CH11231. The theoretical work was supported by the Basque Department of Education, UPV/EHU (Grant No. IT-366-07), the Spanish Ministerio de Ciencia e Innovación (Grant No. FIS2007-66711-C02-00), and the ETORTEK program funded by the Basque Departamento de Industria and the Diputación Foral de Guipúzcoa.

*Corresponding author; mbsalmeron@lbl.gov

- ¹M. J. Gladys, A. A. El-Zein, A. Mikkelsen, J. N. Anderson, and G. Held, *Phys. Rev. B* **78**, 035409 (2008).
- ²M. J. Gladys, A. Mikkelsen, J. N. Andersen, and G. Held, *Chem. Phys. Lett.* **414**, 311 (2005).
- ³P. Cabrera-Sanfelix, A. Arnau, A. Mugarza, T. K. Shimizu, M. Salmeron, and D. Sanchez-Portal, *Phys. Rev. B* **78**, 155438 (2008).
- ⁴A. Mugarza, T. K. Shimizu, P. Cabrera-Sanfelix, D. Sanchez-Portal, A. Arnau, and M. Salmeron, *J. Phys. Chem. C* **112**, 14052 (2008).
- ⁵A. Shavorskiy, M. J. Gladys, and G. Held, *Phys. Chem. Chem. Phys.* **10**, 6150 (2008).
- ⁶D. L. Doering and T. E. Madey, *Surf. Sci.* **123**, 305 (1982).
- ⁷K. Kretzschmar, J. K. Sass, A. M. Bradshaw, and S. Holloway, *Surf. Sci.* **115**, 183 (1982).
- ⁸P. A. Thiel and T. E. Madey, *Surf. Sci. Rep.* **7**, 211 (1987).
- ⁹P. A. Thiel, F. M. Hoffmann, and W. H. Weinberg, *Phys. Rev. Lett.* **49**, 501 (1982).
- ¹⁰P. Cabrera-Sanfelix, D. Sanchez-Portal, A. Mugarza, T. K. Shimizu, M. Salmeron, and A. Arnau, *Phys. Rev. B* **76**, 205438 (2007).
- ¹¹P. J. Feibelman, *Science* **295**, 99 (2002).
- ¹²J. Cerdá, A. Michaelides, M.-L. Bocquet, P. J. Feibelman, T. Mitsui, M. Rose, E. Fomin, and M. Salmeron, *Phys. Rev. Lett.* **93**, 116101 (2004).
- ¹³M. Tatarkhanov, D. F. Ogletree, F. Rose, T. Mitsui, E. Fomin, S. Maier, M. Rose, J. I. Cerdá, and M. Salmeron, *J. Am. Chem. Soc.* **131**, 18425 (2009).
- ¹⁴T. E. Madey and F. P. Netzer, *Surf. Sci.* **117**, 549 (1982).
- ¹⁵K. D. Gibson, M. Viste, and S. J. Sibener, *J. Chem. Phys.* **112**, 9582 (2000).
- ¹⁶B. Narloch, G. Held, and D. Menzel, *Surf. Sci.* **317**, 131 (1994).
- ¹⁷K. L. Kostov, H. Rauscher, and D. Menzel, *Surf. Sci.* **278**, 62 (1992).
- ¹⁸F. M. Hoffmann, M. D. Weisel, and C. H. F. Peden, *Surf. Sci.* **253**, 59 (1991).
- ¹⁹M. Stichler and D. Menzel, *Surf. Sci.* **419**, 272 (1999).
- ²⁰M. Stichler, C. Keller, C. Heske, M. Staufer, U. Birkenheuer, N. Rösch, W. Wurth, and D. Menzel, *Surf. Sci.* **448**, 164 (2000).
- ²¹P. Jakob, M. Stichler, and D. Menzel, *Surf. Sci.* **370**, L185 (1997).
- ²²A. Shavorskiy, T. Eralop, E. Ataman, C. Isvoranu, J. Schnadt, J. N. Andersen, and G. Held, *J. Chem. Phys.* **131**, 214707 (2009).
- ²³H. Pfnür, G. Held, M. Lindroos, and D. Menzel, *Surf. Sci.* **220**, 43 (1989).
- ²⁴G. Kresse and J. Hafner, *Phys. Rev. B* **47**, 558 (1993).
- ²⁵G. Kresse and J. Hafner, *Phys. Rev. B* **49**, 14251 (1994).
- ²⁶G. Kresse and J. Furthmüller, *Phys. Rev. B* **54**, 11169 (1996).
- ²⁷J. P. Perdew, J. A. Chevary, S. H. Vosko, K. A. Jackson, M. R. Pederson, D. J. Singh, and C. Fiolhais, *Phys. Rev. B* **46**, 6671 (1992).
- ²⁸P. E. Blöchl, *Phys. Rev. B* **50**, 17953 (1994).
- ²⁹G. Kresse and D. Joubert, *Phys. Rev. B* **59**, 1758 (1999).
- ³⁰J. Tersoff and D. R. Hamann, *Phys. Rev. Lett.* **50**, 1998 (1983).
- ³¹J. Tersoff and D. R. Hamann, *Phys. Rev. B* **31**, 805 (1985).
- ³²F. Calleja, A. Arnau, J. J. Hinarejos, A. L. V. de Parga, W. A. Hofer, P. M. Echenique, and R. Miranda, *Phys. Rev. Lett.* **92**, 206101 (2004).
- ³³C. Corriol, F. Calleja, A. Arnau, J. J. Hinarejos, A. L. V. de Parga, W. A. Hofer, and R. Miranda, *Chem. Phys. Lett.* **405**, 131 (2005).
- ³⁴T. K. Shimizu, A. Mugarza, J. I. Cerdá, M. Heyde, Y. Qi, U. D. Schwarz, D. F. Ogletree, and M. Salmeron, *J. Phys. Chem. C* **112**, 7445 (2008).
- ³⁵P. Quinn, D. Brown, D. P. Woodruff, T. C. Q. Noakes, and P. Bailey, *Surf. Sci.* **491**, 208 (2001).
- ³⁶C. Stampfl and M. Scheffler, *Phys. Rev. B* **54**, 2868 (1996).
- ³⁷M. A. Henderson, *Surf. Sci. Rep.* **46**, 1 (2002).
- ³⁸M. M. Thiam, T. Kondo, N. Horimoto, H. S. Kato, and M. Kawai, *J. Phys. Chem. B* **109**, 16024 (2005).